DISMA excellence project: T3
Numerical methods for models with high geometric complexity

Dipartimento di Scienze Matematiche
" Giuseppe Luigi Lagrange "
Politecnico di Torino

DISMA
21 Marzo 2018

Outline

- Geometrical complexities: flows in fractured media [20m]
- Geometrical complexities: other applicative problems [5m]
- Up-scaling/homogenization [Chiadò Piat 10m]
- Uncertain Geometries and Uncertainty Quantification Methods [Pieraccini 15m]
- Quasi-static fracture propagation [Zanini 5m]
- FEM-BEM coupling for wave propagation problems in unbounded domains [Falletta 5m]
- Discrete Differential Geometry and Integrable Systems [Manno 15m]
- Tensors, Rank and Manifolds [Carlini 20m]

Other topics of the Task: "a posteriori" error analysis, mesh and time-step adaptivity, wavelets and frames.

Known physical contexts

- Flows and transport in fractured media
- Pore scale fluid flows
- Fracture propagation
- Mechanical behaviour of Fibro-Reinforced materials
- Composite materials
- Fretting (erosion/corrosion under repeated loads)
- Biological problems

Flow in fractured media

Simulation of flow in fractured media is a challenging issue relevant in several critical applications concerning safety assessment of underground exploitation, e.g.:

- aquifers monitoring
- geothermal applications
- oil&Gas enhanced production
- geological storage
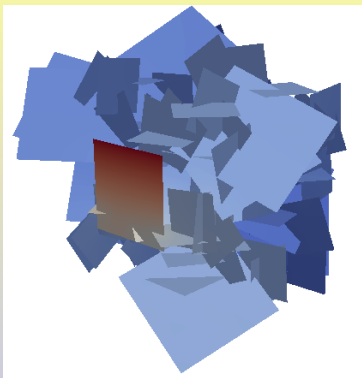- ...

DFN: Discrete Fracture Network

Figure: Example of DFN

- 3D network of intersecting fractures
- Fractures are represented as planar polygons
- Fractures are stochastically generated starting from probabilistic distributions of density, dimension, position, orientation and aspect ratio
- Flow driven by hydraulic head gradients modeled by Darcy law in the fractures
- Flux balance and hydraulic head continuity imposed across trace intersections

Challenges:

- Very large domain: huge computational cost and memory requirements
- Complex domain: difficulties in good quality mesh generation

Motivation

- DFN simulations are largely interesting in those situations in which the discrete nature of the fractures strongly impacts on the directionality of the flow. (No R.E.V Representative Elementary Volume)
- DFN flow simulations are usually applied to simulate the underground displacement of, e.g., a pollutant, water or super-critical carbon dioxide.
- The simulations mainly aim at estimating the flux (including its resulting directionality), the characteristic time, the concentration of a pollutant at specific locations...
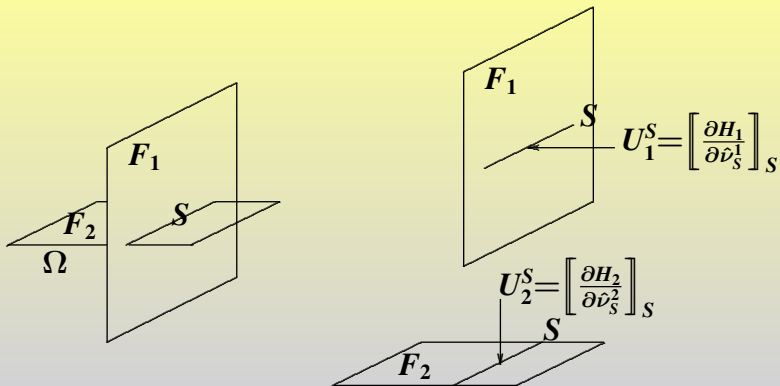
- *Traces*: intersections between fractures, denoted by S. Each trace is shared by exactly *two* fractures $S = \bar{F}_i \cap \bar{F}_j$ and $I_S := \{i, j\}$;
- For each trace $S \in \mathcal{S}$ on the fracture F_i, let use denote by

$$U_i^S := \left[\!\!\left[\frac{\partial H_i}{\partial \hat{\nu}_S^i} \right]\!\!\right]_S \quad U_i^S \in \mathcal{U}^S \subseteq \mathbf{H}^{-\frac{1}{2}}(S)$$

the flux entering in the fracture through the trace S, and $U_i \in \mathcal{U}^{\mathcal{S}_i}$ the tuple of fluxes $U_i^S \ \forall S \in \mathcal{S}_i$.

- $\forall i \in I$;

let us set b.c.: $\partial F_i = \Gamma_{iN} \cup \Gamma_{iD}$ with $\Gamma_{iN} \cap \Gamma_{iD} = \emptyset$ and $\Gamma_{iD} \neq \emptyset$ *(for ease of exposition)*,

and solve the problem: find $H_i \in \mathbf{H}_D^1(F_i)$ and $U_i \in \mathcal{S}_i$ such that:

$$(\mathbf{K_i} \nabla H_i, \nabla v) = (q_i, v) + \langle U_i, v_{|\mathcal{S}_i} \rangle_{\mathcal{U}^{\mathcal{S}_i}, \mathcal{U}^{\mathcal{S}_i{}'}} \qquad \boxed{\blacktriangleright J(U)} \boxed{\blacktriangleright J_\alpha(U)}$$

$$+ \langle G_{iN}, v_{|\Gamma_{iN}} \rangle_{\mathbf{H}^{-\frac{1}{2}}(\Gamma_{iN}), \mathbf{H}^{\frac{1}{2}}(\Gamma_{iN})}, \quad \forall v \in V_i = \mathbf{H}_{0,D}^1(F_i)$$

- $\forall S \in \mathcal{S}$ prescribe matching conditions

$$H_{i|S} - H_{j|S} = 0, \quad \text{for } i, j \in I_S,$$

$$U_i^S + U_j^S = 0, \quad \text{for } i, j \in I_S.$$

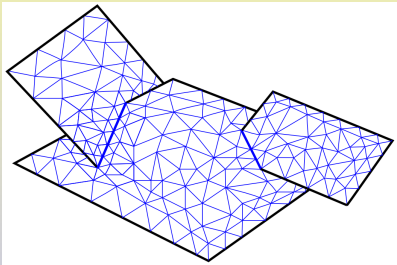*"Continuity" of the hydraulic head provides* $H \in V = \mathbf{H}_D^1(\mathcal{D})$.
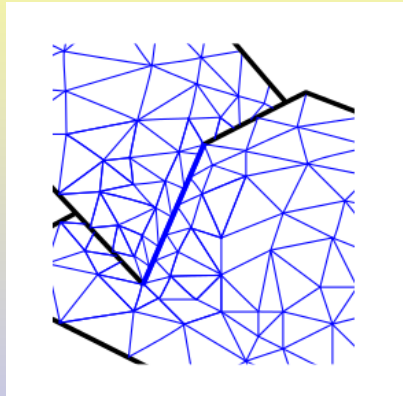
Figure: Totally conforming mesh

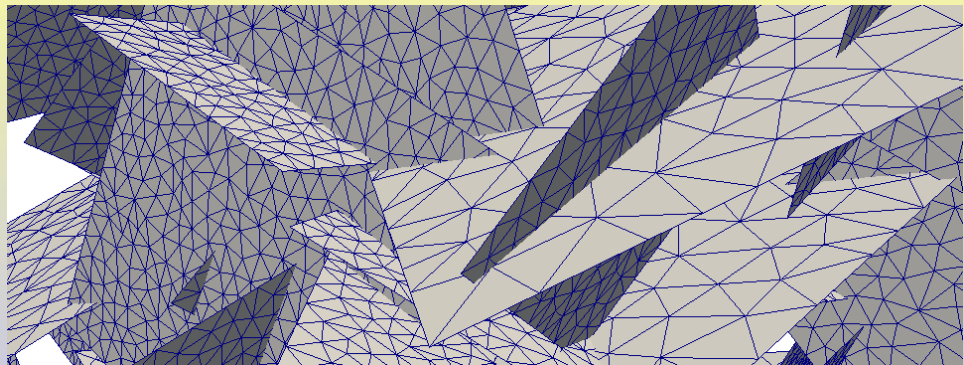Figure: Partially conforming mesh

Figure: Non-conforming mesh on a 120 fracture DFN

B. S., Pieraccini S., Scialò S., 2013 *A PDE-constrained optimization formulation for discrete fracture network flows*.

Instead of solving the differential problems on the fractures coupled by the corresponding matching conditions we look for the solution as the minimum of **a PDE constrained quadratic optimal control problem**, the variable U **being the control variable**. Let us define the differentiable functional $J : \mathcal{U} \to \mathbb{R}$ as

$$J(U) = \sum_{s \in \mathcal{S}} \left(||H_i(U_i)_{|s} - H_j(U_j)_{|s}||^2_{\mathcal{H}^s} + ||U_i^S + U_j^S||^2_{\mathcal{U}^s} \right) \quad \boxed{\blacktriangleright H(U)}$$

We look for the **control variable U providing the minimum of the functional $J(U)$ constrained by the equation for H_i on each fracture**.

In order to consider **more general matching conditions** we can plug in the functional the **squared norm of the residual of the new matching conditions**.

With this definition of the control variables **the differential problem on each fracture has to be well posed**.

- Introduce a mesh on each fracture, completely **independent of the meshes on the intersecting fractures**.
- Let us further define on this mesh a finite element-like discretization h for H (FEM, XFEM, VEM, ...), different methods on different fractures can be combined as well.
- Introduce also a discretization u for the control variable U, **on the traces of each fracture independently**.
- The minimization of the functional is performed by an **iterative conjugate gradient** approach.
- The gradient method requires the solution of **many local small problems.**
- With arbitrary meshes **the minimum of the functional is not null**.

$\Rightarrow$ Efficient and Reliable Meshes on the fractures and on the traces can be pursued by "a posteriori" error analysis and mesh adaptivity.

B. S., Pieraccini S., Scialò S., 2013, *On simulations of discrete fracture network flows with an optimization-based extended finite element method.*

B. S., Pieraccini S., Scialò S., 2014, *Towards effective flow simulations in realistic Discrete Fracture Networks.*

Benedetto M.F., B. S., Pieraccini S., Scialò S., 2014, *The Virtual Element Method for discrete fracture network simulations.*

B. S., Borio A., 2017, *A Residual A Posteriori error estimate for the Virtual Element Method.*

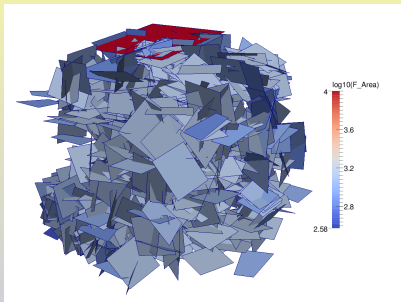Canuto C., Nochetto R., Stevenson R., Verani M., 2017, *Convergence and optimality of hp-AFEM.*

Figure: 3D view of DFN 709 Fractures, 3939 Traces, Area: $376m^2 - 10^4m^2$
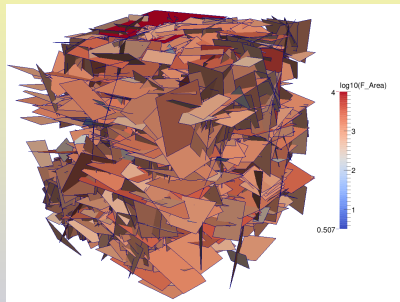

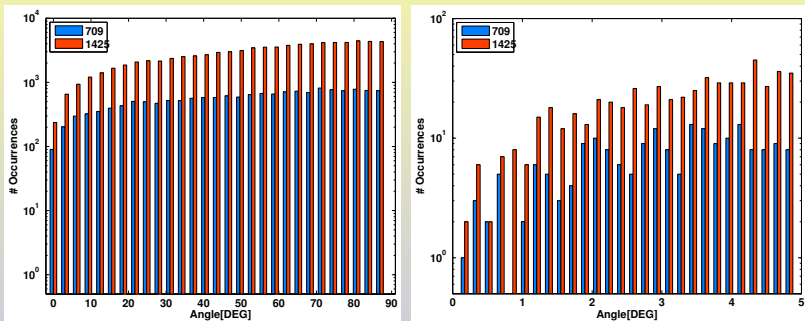Figure: 3D view of DFN 1425 Fractures, 13086 Traces, Area: $3.2m^2 - 10^4m^2$

Figure: DFN709 and DFN1425. Left: distribution of angles between pairs of intersecting traces in the same fracture: $0.26°$-$90°$; right: zoom of lower values.
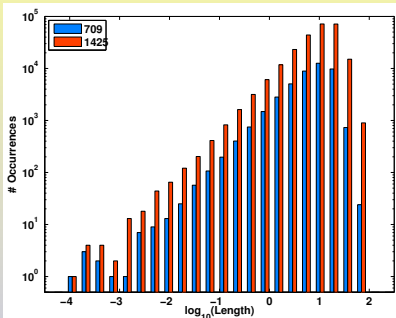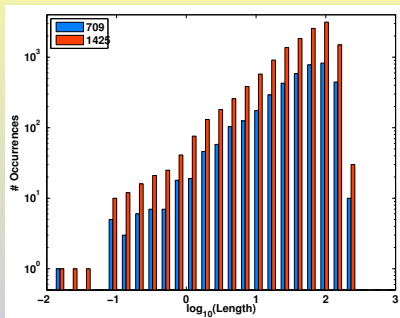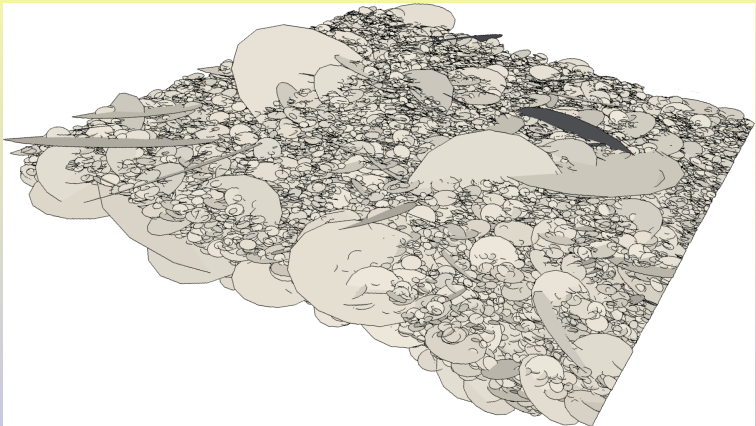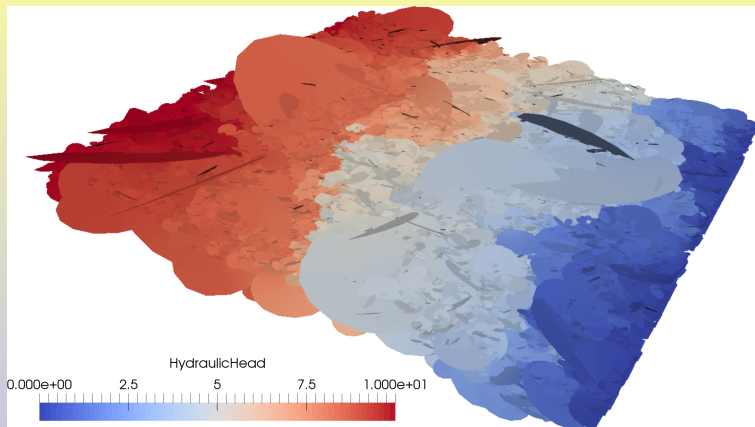
Figure: DFN709 and DFN1425: distribution of trace lengths: $1.6cm - 260m$ (left) and of distances between couples of non-intersecting traces in the same fracture: $0.12mm - \sim 100m$ (right)

Fractures	Connected	Traces	Mesh×Fracture
32,224	32,212	60,778	100

DOFs	Residual	Total Time	Memory
$4.15 \cdot 10^6$	$1 \cdot 10^{-6}$	≈ 10 min	12 GB

Unsteady advection-diffusion in DFNs

$$\frac{\partial \mathcal{C}}{\partial t} - \nabla \cdot \mu \nabla \mathcal{C} + \beta \cdot \nabla \mathcal{C} = 0, \qquad \text{a.e. in } \mathcal{D} \times (0, T]$$

The optimization framework can be modified in order to compute the dispersion of a passive scalar $\mathcal{C}(t, x)$ in the DFN.

Let us re-define the variable $U_i^S \in \mathbf{H}^{-\frac{1}{2}}(S)$ as:

$$U_i^S = \left[(\mu_i \nabla \mathcal{C}_i) \cdot n_S^i + \beta_i \cdot n_S^i \mathcal{C}_i \right]_S + \alpha \, \mathcal{C}_{i|S}.$$

Let us denote by

- μ_i the diffusivity/dispersivity of the pollutant in the fracture;
- $\beta_i = -\mathbf{K}_i \nabla H_i / e_i$ the restriction of Darcy velocity β to F_i computed solving the flow problem by means of the optimization approach;
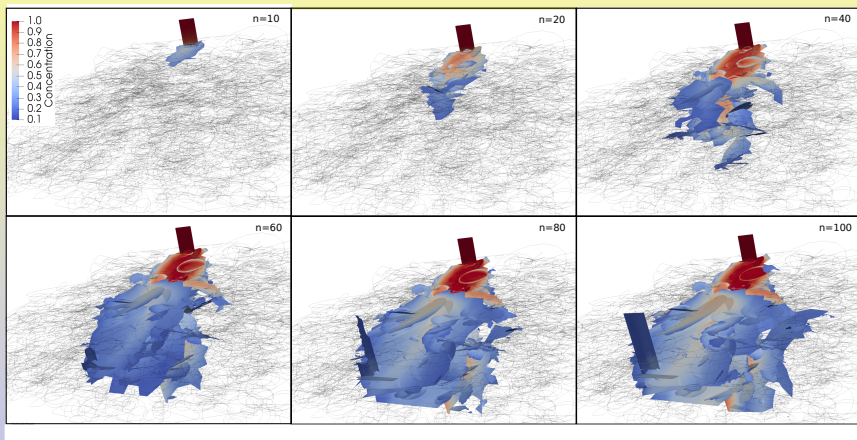- $\alpha > 0$ a constant parameter for "Dirichlet boundary conditions".

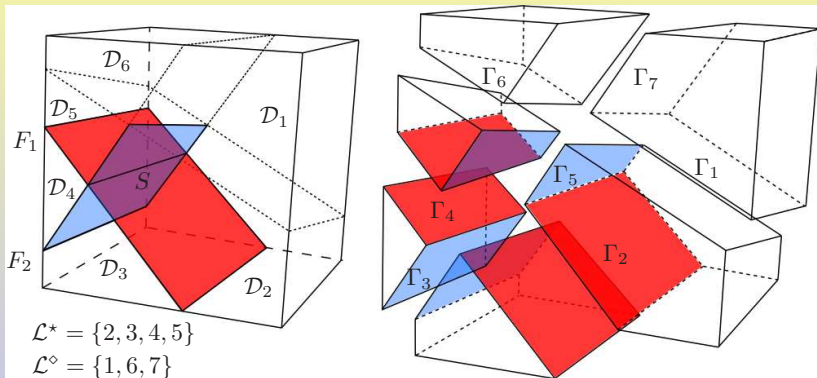Figure: Transport in a complex DFN

Matrix-Fracture coupling

Figure: **Geometry and notations**

B. S., Pieraccini S., Scialò S., (2017), *Flow simulations in porous media with immersed intersecting fractures.*

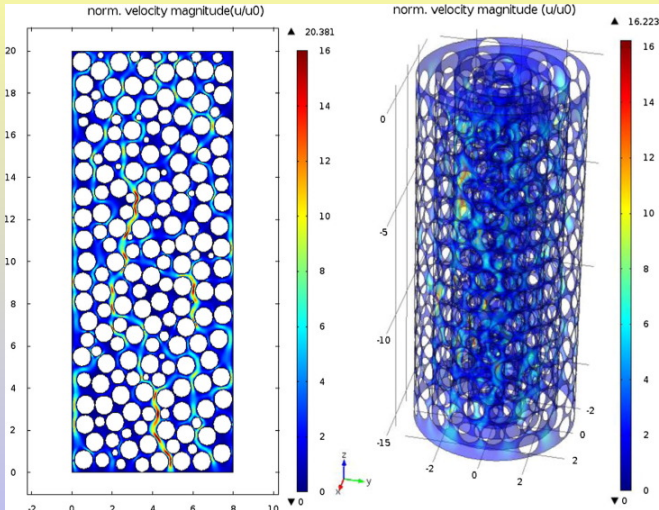## Estimation of hydraulic properties by inter-pore flows

Figure: Granular material
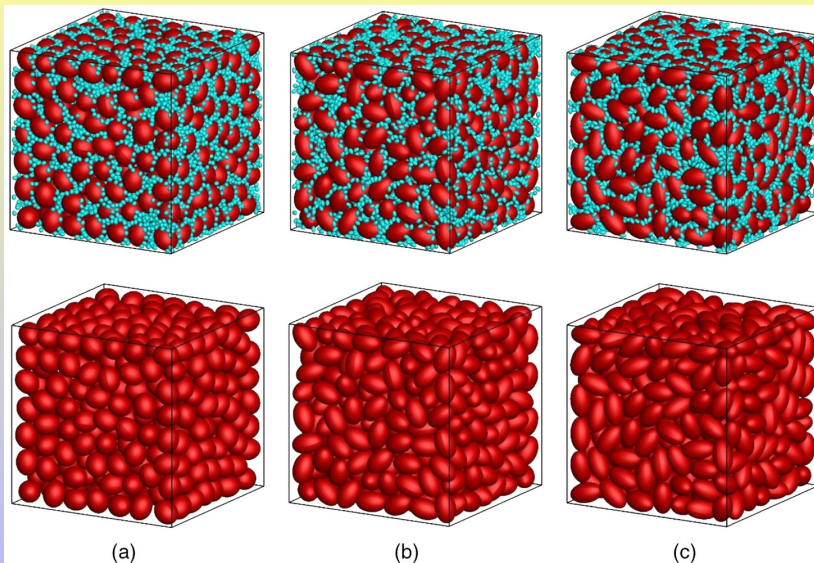
Porosity estimation by inter-pore flows

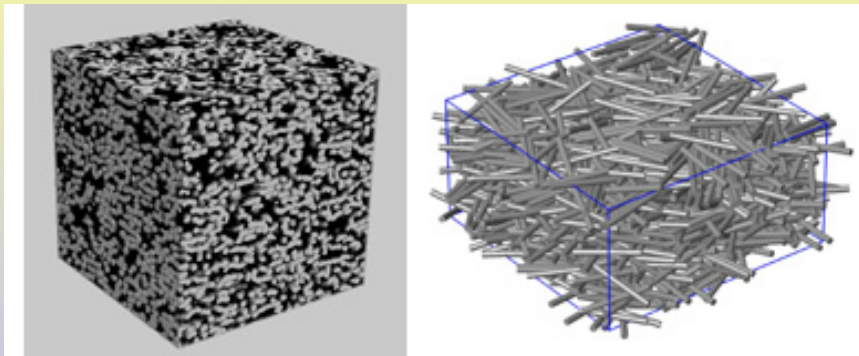(a)   (b)   (c)

Figure: Granular material

Figure: Granular and Fibrous material

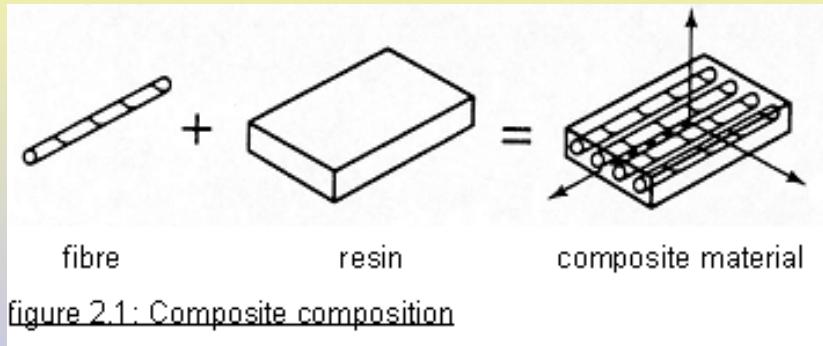## Mechanical behaviour of fibroreinforced materials
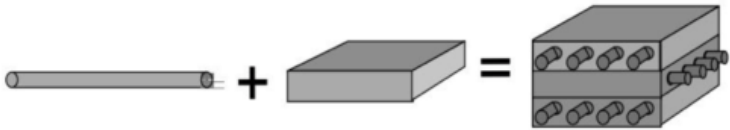

fibre   resin   composite material

figure 2.1: Composite composition

Figure: Fibro-reinforced material

Fiber/Filament Reinforcement

Matrix

Composite

- High strength
- High stiffness
- Low density
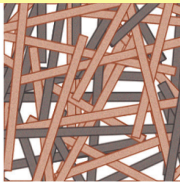
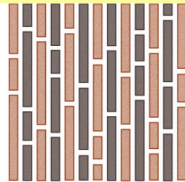- Good shear properties
- Low density

- High strength
- High stiffness
- Good shear properties
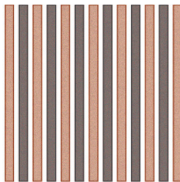- Low density
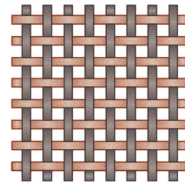
Figure: Fibro-reinforced material

Discontinuous and randomly oriented

Discontinuous and aligned

Continuous and aligned

Fabric

Figure: Fibro-reinforced material
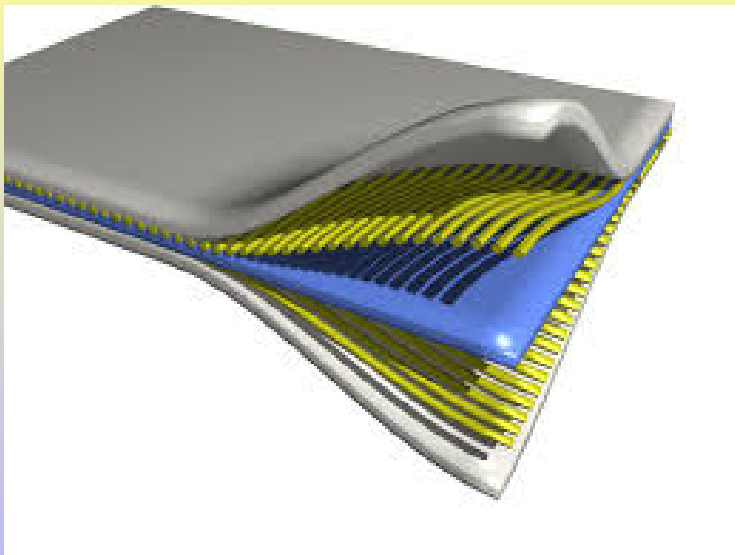
Mechanical behaviour of composite materials

Figure: Layered material
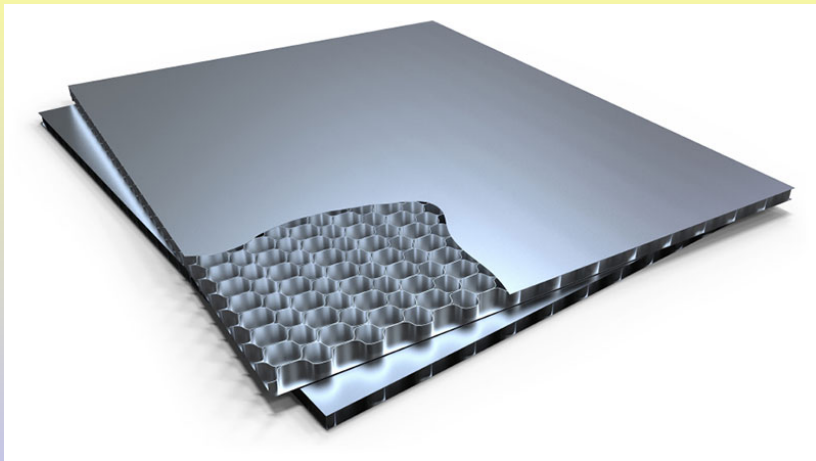
Figure: Composite material
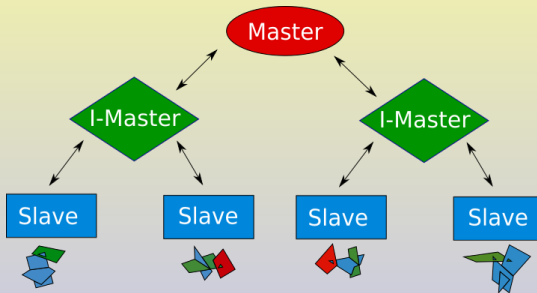
DFN Parallel decomposition (Metis)

Figure: Multi-Master-Slave DFN decomposition and communication

Message Passing Interface (F. Vicini)

Figure: DFN: 1K, 2K, 4K, 8K, 16K, 32K, 64K, 128K, 256K fractures

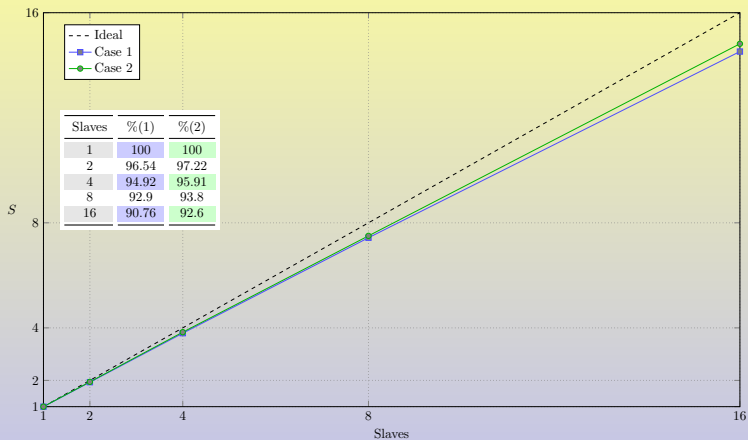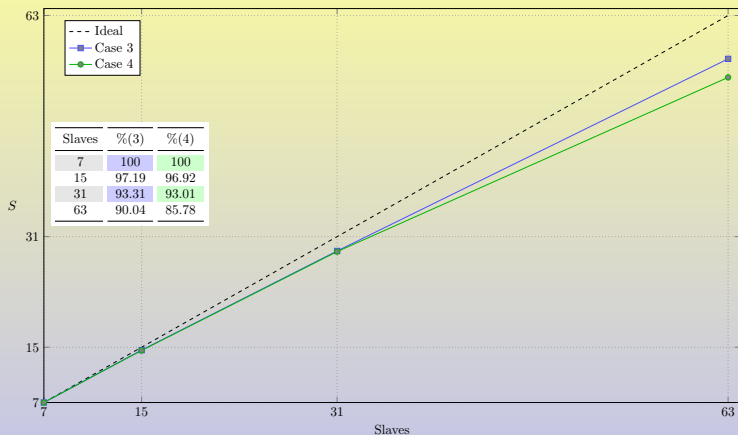Figure: Parallel scalability (use of a single core per node)

Slaves	%(3)	%(4)
7	100	100
15	97.19	96.92
31	93.31	93.01
63	90.04	85.78

Figure: Parallel scalability (use of 8 core per node)

Nvidia CUDA (A. D'Auria)

Table: Number of fractures and traces for each DFN

DFN	#Fractures	#Traces	Min #Tr	**Max #Tr**	$\frac{\#Traces}{\#Fractures}$
1425	1425	13086	1	92	9.18
4937	4937	346196	1	**1040**	70.12
12000	12000	991638	18	**1607**	82.64
40728	33334	78713	1	22	2.36

Table: DFN12000: degrees of freedom on the fractures and traces

#Tri	DegF	DegT	**hDofs**	**uDofs**	$\frac{\text{uDofs}}{\text{hDofs}}$
50	P1	P0	583067	13231759	22.69
100	P1	P0	1099632	18187858	16.54
50	P1	P1	583067	15215035	26.09
100	P1	P1	**1099632**	**20171134**	18.34

Simulations performed by: NVIDIA GTX TITAN X

Table: DFN12000: Speed-up for different discretizations

| #Tri	DegT	Cpu (s)	Gpu (s)	SpUp
50	P0	735.33	48.46	15.17
100	P0	1120.59	72.13	15.53
50	P1	1201.51	61.87	19.42
100	P1	1586.14	83.23	19.06

Biomedical applications

The numerical tools developed allow:

- the treatment of complex geometries characterized by the presence of numerous interfaces
- the coupling between problems of different dimensions: typically 2D-1D; 3D-2D. Extension to 3D-1D
- the coupling between different operators
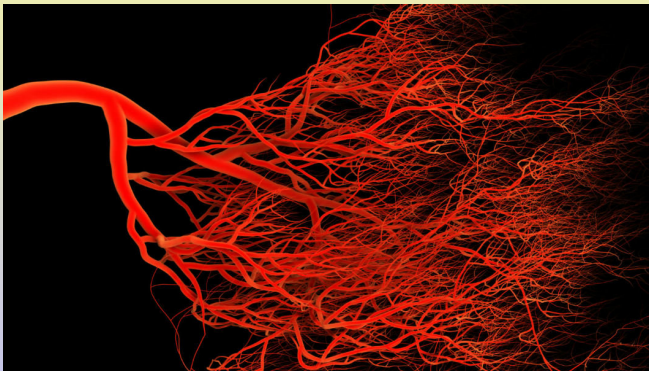- the use of uncertainty quantification techniques

The key point is that the problem in the complex domain is reduced to many problems on **very simple** domains with suitable additional coupling conditions

Bones
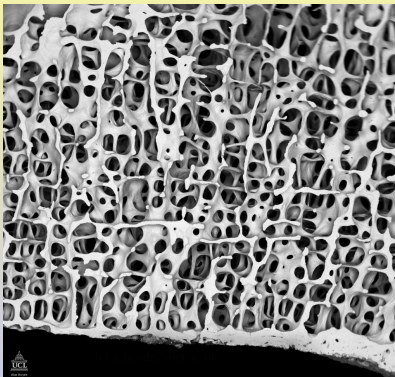
Vessels-Tissue interaction

Brain